Chapter 1

Multilayer Modeling of Skin Color and Translucency

Gladimir V. G. Baranoski,[a] Tenn F. Chen,[a] and Aravind Krishnaswamy[b]

[a]*University of Waterloo,*
200 University Ave. West, Waterloo, Ontario, N2L 3G1, Canada
[b]*Google Inc.,*
1600 Amphitheatre Parkway, Mountain View, CA 94043, USA
gvgbaran@curumin.cs.uwaterloo.ca

1.1 Introduction

The computer modeling of skin appearance has a wide range of applications, from the generation of realistic images for educational and entertainment purposes to the screening of medical conditions and the assessment of the efficacy of sunscreens and cosmetics. Skin appearance attributes, such as color and translucency, result from complex light interaction processes. In order to simulate these processes and obtain reliable predictions about skin appearance attributes, it is necessary to take into account the biophysical properties of the different skin tissues such as thickness, refractive index, and the presence of light absorbers and scatterers. Although the main skin tissues are normally represented by layers during light transport simulations, the number of skin layers and

Computational Biophysics of the Skin
Edited by Bernard Querleux

ISBN 978-981-4463-84-3 (Hardcover), 978-981-4463-85-0 (eBook)
www.panstanford.com

the level of detail employed to characterize them may vary among the different skin multilayer models available in the literature.

In this chapter, we concisely address these modeling efforts from a practical perspective. We start with an outline of relevant radiometric concepts related to the measurement of appearance of skin specimens, followed by an overview of the different approaches normally used to simulate light propagation and absorption within skin multilayer modeling frameworks. We then discuss predictability and reproducibility guidelines that should be followed so that skin appearance models can be effectively employed in interdisciplinary investigations and applications that involve the high fidelity simulation of skin color and translucency. During this discussion, we briefly examine a biophysically based spectral model of light interaction with human skin (BioSpec [1]) that has been employed in different application domains, from realistic image synthesis [2] to biomedical optics [3] and pattern recognition [4]. This particular case study is used to illustrate issues related to model development and evaluation procedures, as well as current trends involving the reproducibility of model predictions and code transparency. We close the chapter with an outlook on open research avenues that can lead to future advances in the predictive modeling of skin appearance attributes.

1.2 Measurement of Skin Appearance

The group of measurements necessary to characterize the appearance of a given material is called its measurement of appearance [5]. These measurements involve the spectral and the spatial energy distribution of the light propagated by the material. The variations in the spectral distribution of the propagated light are responsible for appearance attributes such as hue, lightness, and saturation, while changes in the spatial distribution of the propagated light affect appearance characteristics such as glossiness and translucency.

The spectral energy distribution of the propagated light is usually measured in terms of reflectance and transmittance. There are nine different representations of reflectance and transmittance. These representations depend on the incident and propagated (collected) light geometries, which are designated as directional, conical, and hemispherical [6].

The spatial patterns of light distribution are represented by the bidirectional scattering-surface distribution function (BSSDF) [6]. The BSSDF is considered to be a difficult function to measure, store and compute due to its dependency on four parameters: the incidence direction, the propagation direction, the wavelength of the incident light, and the position on the target surface [6]. Hence, for practical purposes, the bidirectional scattering distribution function (BSDF, or simply BDF) is often employed to describe the light scattering behavior of complex biological materials such as human skin.

The BDF assumes that the point of light incidence and the point of light propagation by the material are separated by a negligible distance. This function can be further decomposed into two components: the bidirectional reflectance distribution function (BRDF) and the bidirectional transmittance distribution function (BTDF).

Although the spectral and spatial distributions of light propagated by human skin can be measured separately, they work together to give us the different visual impressions of this biological surface. More specifically, incident light interacts with a skin specimen characterized by a BSSDF, and it may be directionally propagated toward our eyes. Upon reaching our visual system, the incoming light is translated to appearance attributes such as color, glossiness, and translucency. Hence, the appearance of human skin depends on spectral and spatial light distributions, which, in turn, are controlled by the optical properties of biological structures (e.g., cells, organelles, and fibers) present in the cutaneous tissues. These structures are directly associated with the processes of light absorption and scattering within the skin layers, whose histological and optical complexity determine the wide range of spectral signatures and scattering profiles found in the human population.

1.3 Light Transport Simulation Approaches

A large number of multilayered models have been developed for the simulation of light interactions with human skin. Although these models employ the same intuitive concept of layers to represent the cutaneous tissues, their formulation is usually tailored to their target applications. Typically, models developed for biomedical

applications provide as output the spectral power distribution of skin tissues, while models developed for image synthesis applications provide as output spatial power distribution quantities [2]. In order to obtain these modeled quantities, different light transport simulation approaches can be applied, and no single approach is superior in all the cases. The selection of a given approach is usually determined by the requirements of the application at hand. In this section, we outline the two major groups of simulation approaches, namely deterministic and stochastic, employed in the modeling of skin appearance attributes. Combinations of elements of these two groups may be classified as belonging to a third group of hybrid approaches. Although the following presentation is supported by selected key examples, the reader interested in a broader review of light transport simulations approaches used in this area is referred to comprehensive texts on this topic [2,7,8].

1.3.1 Deterministic Simulations

The deterministic simulation approaches used in the modeling of skin appearance attributes rely on the explicit solution of light transport equations through standard numerical techniques. For example, within the Kubelka–Munk theory framework [9], differential equations are used to describe light transport in a medium using as parameters its scattering and absorption coefficients. In skin optics, the Kubelka–Munk theory was initially applied to specific skin tissues. For example, Anderson and Parish [10] developed a model that employed the Kubelka–Munk theory to compute absorption and scattering coefficients for the dermis tissues. Wan et al. [11] extended this model to compute the absorption and scattering coefficients for the epidermis tissues, taking into account both collimated and diffuse incident irradiance. Later on, Doi and Tominaga [12] presented a model that considers the skin composed of two layers representing the epidermis and dermis tissues. They applied the Kubelka–Munk theory to both layers. More recently, the Kubelka–Munk theory has been employed in the modeling of skin appearance attributes for image synthesis applications [13]. Although models based on the Kubelka–Munk theory cannot be considered comprehensive models of optical radiation transfer since they lack a more detailed analysis of the

structure and optical properties of the different skin tissues, their relative simplicity makes them competitive candidates for model inversion procedures used to derive tissue optical parameters from reflectance and transmittance measurements.

Photon propagation in optically turbid media, such as skin tissues, can be described by the time and energy independent equation of radiative transport known as the Boltzmann photon transport equation [14]. The diffusion theory can be seen as an approximate solution to this equation [15]. For example, Farrell and Patterson [16] proposed a model based on the diffusion theory to be used in the noninvasive determination of the absorption and scattering properties of mammalian tissues. Their model incorporates a photon dipole source approximation in order to satisfy the tissue boundary conditions, namely light being propagated from a tissue from a point different from the incidence point, and the presence of thin layers of dirt, blood or other fluids on the surface of the tissue under investigation. Models based on the diffusion theory [17] are amenable to analytic manipulation and relatively easy to use. However, it has been stated that when the absorption coefficient of a turbid medium is not significantly smaller than the scattering coefficient, the diffusion theory provides a poor approximation for the photon transport equation [18–20]. Accordingly, it can be successfully applied only when scattering events are more probable than absorption events. In the case of mammalian tissues, this condition is observed in the red and near infrared regions of the light spectrum [21]. For this reason, in the biomedical field, models based on the diffusion theory are usually employed to support investigations involving red lasers [15,22]. Nonetheless, in the computer graphics field, the diffusion theory has been employed to render believable images of human skin [23,24].

When more reliable solutions to the radiative light transport equation in biological tissues are required, more robust methods, such as the adding-doubling method and the discrete ordinate method, can be used. The adding-doubling method [7,25] requires that the reflectance and transmittance of two identical homogeneous thin layers to be known. They are used to compute the reflectance and transmittance of another layer formed by the juxtaposition of these two individual layers. Once the transmittance and reflectance of this paired layer are known, the reflectance and transmittance

of a target layer can be computed by repeating this process, i.e., doubling the ensemble of paired layers, until the thickness of the resulting multilayered structure matches the thickness of the target layer.

The discrete ordinate method divides the radiative transport equation into *n* discrete fluxes to obtain *n* equations with *n* unknowns. These equations are then solved using numerical techniques. For example, Nielsen et al. [26] have proposed a skin model composed of five epidermal layers of equal thickness, a dermal layer, and a subcutaneous layer. The subdivision of the epidermis into five layers allowed Nielsen et al. [26] to simulate different contents and size distributions of the melanin-containing organelles (melanosomes). The radiative light transport equation associated with this layered model is then solved using the discrete ordinate algorithm proposed by Stamnes et al. [27] for the simulation of radiative transfer in layered media. This approach is feasible when the phase function (used to describe the bulk scattering of the material under investigation) can be expressed as a sum of Legendre polynomials [28]. For highly asymmetric phase functions, it is necessary to consider a large number of fluxes, which may result in a numerically ill-conditioned system of equations [7].

1.3.2 Stochastic Simulations

Models based on stochastic simulation approaches rely on Monte Carlo methods [29] to account for the different optical phenomena affecting light transport within the skin tissues. These methods are usually applied in conjunction with ray optics techniques. More specifically, the light transport processes are simulated as random walks in which the photon (ray) histories are recorded as they are scattered and absorbed within a given skin layer.

Monte Carlo models are extensively used in skin related applications in image synthesis, biomedicine, colorimetry, and pattern recognition, either online (e.g., to determine skin optical properties and other biophysical attributes through inversion procedures) or offline (e.g., to evaluate the effectiveness of modeling frameworks based on deterministic approaches). For example, Shimada et al. [30] proposed a regression analysis algorithm to determine melanin and blood concentration in human skin. In

their investigation, they applied the modified Beer–Lambert law [2] and considered three-layered (epidermis, dermis and subcutaneous tissue) skin phantoms. To assess the accuracy of their predictions, they employed a general-purpose Monte Carlo algorithm for light transport in multilayered tissues (Monte Carlo modeling of light transport in multi-layered tissues, or simply MCML) developed by Wang et al. [31]. The same algorithm was employed by Nishidate et al. [32] in their regression analysis investigation aimed at the estimation of melanin and blood concentration in the human skin. However, Nishidate et al. [32] considered two-layered (epidermis and dermis) skin phantoms, and employed the MCML model not only to verify the fidelity of their predictions, but also to derive input data from a number of MCML simulated absorption spectra.

Monte Carlo methods can provide flexible and yet rigorous solutions to light transport within skin tissues [31]. However, many trials (sample rays) are required to determine the overall local light transport behavior of a given skin specimen. For this reason, Monte Carlo models are often employed offline to generate data or to assess the accuracy of predictions provided by other models (e.g., [21,33]). Although most Monte Carlo models share a similar mathematical formulation, key aspects distinguish one model from another and affect the overall accuracy of their predictions. These aspects include the level of abstraction used to represent the skin tissues (e.g., number of layers) and their parameter space. In addition, the correctness of their simulation algorithms is bound by the use of proper representations for the mechanisms of scattering and absorption of photons (rays) as well as the reliability of their input data. Hence, the use of a Monte Carlo model to generate input or evaluation data to another model is scientifically sound only if the predictions provided by the reference Monte Carlo model have been properly evaluated in the first place. It is worth noting that this information is often omitted in related publications.

1.4 Practical Guidelines

Multilayered skin models are usually developed for specific applications. For example, they can be designed to simulate variations

in the reflectance of skin specimens as responses to physiological changes caused by pathological conditions, or to add glossiness effects on the face of a virtual character. However, it is possible to develop models that can be used in different fields as long as a set of practical guidelines is taken into account. Ideally, such models should enable the computation of spectral and spatial readings for the light propagated by a given skin specimen. More importantly, these models need to be predictive, i.e., their simulation algorithms need to be controlled by biophysically meaningful parameters, and their predictions should be quantitatively and qualitatively evaluated through comparisons with actual measured data. Furthermore, the results provided by such models should be fully reproducible, which requires the complete disclosure of the data and computer code used in the simulations. After all, the reproduction of research findings is one of the fundamental criteria employed to assess scientific contributions.

To date, only a handful of light transport models fulfill these guidelines [3]. A noteworthy exception to this trend is the biophysically based spectral model of light interaction with human skin (BioSpec [1]), which has been used not only in realistic image synthesis applications [2], but also in biomedical applications [3,4]. In the remainder of this section, we provide an overview of BioSpec, and use this model as a case study to illustrate the feasibility of the practical guidelines mentioned above.

1.4.1 BioSpec Model Overview

The BioSpec model employs Monte Carlo techniques to simulate light interactions with human skin. Within the BioSpec framework, this organ is considered to be composed of four main layers, namely stratum corneum, epidermis, papillary dermis, and reticular dermis (Fig. 1.1). Accordingly, the BioSpec parameter space includes the refractive index and thickness of each of these layers as well as the specific absorption coefficient, concentration and volume fraction of their main pigments (eumelanin, pheomelanin, oxyhemoglobin, deoxyhemoglobin, methemoglobin, sulfhemoglobin, carboxihemoglobin, β-carotene, and bilirubin). In addition, the aspect ratio of the skin surface folds is also included in the model parameter space along with the refractive index and the diameter of the collagen fibers present in the dermal layers.

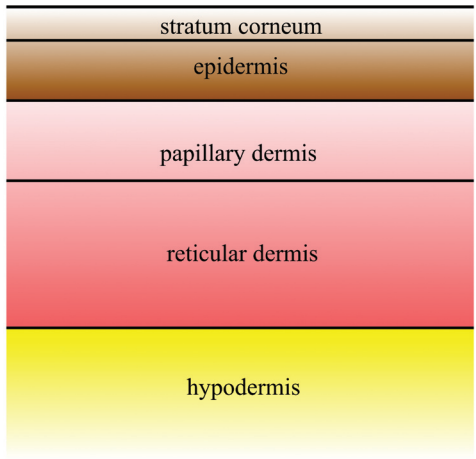

Figure 1.1 Diagram depicting the skin layers considered by the BioSpec model.

The propagation of light within the skin layers is simulated by the BioSpec model as a random walk process (that relies on the generation of random numbers ξ_j, for $j = 1, 2, \ldots, 9$, uniformly distributed in the interval [0, 1]) using ray optics. In this random walk process, the transition probabilities are associated with Fresnel coefficients computed at each interface between the layers, and the termination probabilities are determined by the ray free path length.

Once a ray impinges on the skin surface, it can be reflected back to the environment or transmitted into its internal tissues. In the former case, the distribution of the reflected light is computed taking into account the aspect ratio, denoted by σ, of the skin surface folds. As the surface folds become flatter (lower σ), the reflected light becomes more specular. In order to account for this change in the light reflection behavior, the reflected rays are perturbed using angular displacements obtained from the surface-structure function proposed by Trowbridge and Reitz [34], which represents rough air–material interfaces using microareas randomly curved. These displacements are given in terms of a polar perturbation angle:

$$\theta_s = \cos^{-1}\left[\left(\left(\frac{\sigma^2}{\sqrt{\sigma^4 - \sigma^4\xi_1 + \xi_1}} - 1\right)b\right)^{1/2}\right], \tag{1.1}$$

where b corresponds to $1/(\sigma^2 - 1)$. The corresponding azimuthal perturbation angle ϕ_s is given by $2\pi\xi_2$.

If the ray is transmitted into the skin, then it can be reflected and refracted multiple times within the skin layers before it is either absorbed or propagated back to the environment through the air/stratum corneum interface. In the stratum corneum and epidermis, the scattering of the propagated ray is simulated using angular displacements measured by Bruls and van der Leun [35].

Every ray transmitted into one of the dermal layers is initially tested for Rayleigh scattering [36]. If the test fails or the ray has already been bounced off one of the dermal interfaces, then the ray is randomized around the normal direction using a warping function based on a cosine distribution in which the polar perturbation angle, α_c, and the azimuthal perturbation angle, β_c, are given by

$$(\alpha_c, \beta_c) = (\cos^{-1}((1 - \xi_3)^{1/2}), 2\pi\xi_4). \tag{1.2}$$

In order to perform the Rayleigh scattering test, the spectral Rayleigh scattering amount, $S(\lambda)$, is computed using the appropriate expression for Rayleigh scattering involving particles [36]. Next, a random number ξ_5 is generated. If $\xi_5 < 1 - e^{-S(\lambda)}$, then the ray is scattered using an azimuthal perturbation angle, β_R, given by $2\pi\xi_6$, and a polar perturbation angle, α_R, obtained using the following rejection sampling algorithm based on the Rayleigh phase function [36]:

```
do      α_R = πξ_7
        χ = 3ξ_8/2
while   (χ > 3√6(1 + cos²α_R)sinα_R/8)
```

Since the subcutaneous tissue is a highly reflective medium, it is assumed that light impinging on the reticular dermis/hypodermis interface is reflected toward the upper layers.

Once a ray has been scattered in a given layer, it is probabilistically tested for absorption. This test consists in estimating the ray free path length using a formulation based on the Beer–Lambert law [2]. Accordingly, the ray free path length, $p(\lambda)$, is computed using the following expression:

$$p(\lambda) = -\frac{1}{\mu_i(\lambda)}\ln(\xi_7)\cos\theta, \tag{1.3}$$

where θ corresponds to the angle between the ray and the specimen's normal, and $\mu_i(\lambda)$ represents the total absorption coefficient of a given layer *i*. If $p(\lambda)$ is greater than the thickness of the layer, then the ray is propagated. Otherwise, it is absorbed.

The total absorption coefficient, $\mu_i(\lambda)$, of a given layer *i* accounts for the specific absorption coefficient (s.a.c.) and the concentration of the pigments present in this layer such as the eumelanin and pheomelanin found in the epidermis. These specific absorption coefficients may be incorporated into the model directly if their values are available. Otherwise, they are calculated using the spectral molar extinction coefficients, ε, and molar weights, ω, of the organic absorbers. The expression used to compute the s.a.c. of an absorber *j* is given by

$$s_j(\lambda) = \frac{\varepsilon_j(\lambda)}{\omega_j}\ln 10. \tag{1.4}$$

Note that the factor of ln10 in Eq. 1.4 is needed to convert from an absorbance value (molar extinction) to a specific absorption coefficient.

1.4.2 Predictability

The BioSpec design is based on a first-principles strategy in which the simulations are controlled by the fundamental properties of a given skin specimen such as the contents of individual absorbers. The default values assigned for these biophysically meaningful parameters are selected within valid ranges reported in the literature. Accordingly, the radiometric predictions provided by the BioSpec model are amenable to evaluation through comparisons with actual measured data [2]. For example, modeled spectral curves can be obtained using a virtual spectrophotometer [37], and compared with measured ones. This procedure is illustrated in Fig. 1.2, which depicts comparisons of modeled and measured reflectance curves for two skin specimens with different levels of pigmentation, namely a lightly pigmented (LP) and a moderately pigmented (MP) specimen. In these comparisons, the measured

curves correspond to measurements provided by Vrhel et al. [38]. These measurements were made available in a spectra database at the North Carolina State University (NCSU spectral files 113 and 82, respectively). The pigmentation parameters used to generate the modeled curves (Table 1.1) were selected based on the skin type description of the actual specimens provided in the NCSU spectra database and the corresponding ranges for these parameters available in the literature [39]. The values assigned for the remaining BioSpec parameters employed in the computation of the modeled curves were gathered from related scientific publications (Table 1.2). Both sets of modeled and measured curves were obtained considering the same angle of incidence (45°).

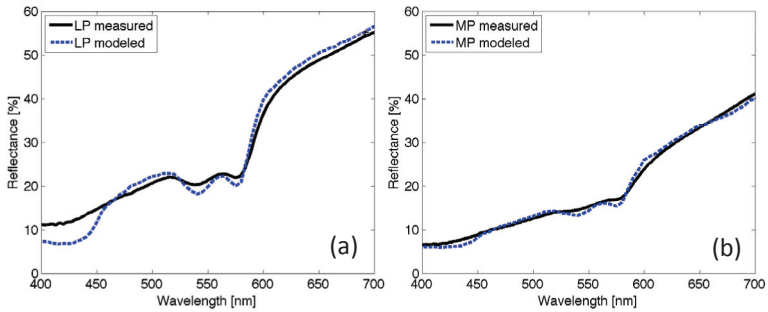

Figure 1.2 Comparisons of modeled directional-hemispherical reflectance curves (obtained using the BioSpec model [1] and considering specimens characterized by the parameters provided in Tables 1.1 and 1.2) with measured directional-hemispherical reflectance curves provided by Vrhel et al. [38]. All modeled and measured curves were obtained considering an angle of incidence equal to 45°. (a) Lightly pigmented (LP) specimen. (b) Moderately pigmented (MP) specimen.

Table 1.1 Skin pigmentation–related parameters employed by BioSpec model to characterize a lightly pigmented (LP) specimen and a moderately pigmented (MP) specimen

Parameter	LP	MP
Percentage of epidermis occupied by melanosomes	1.6%	3.6%
Percentage of papillary dermis occupied by blood	0.8%	0.6%
Percentage of reticular dermis occupied by blood	0.8%	0.6%

Table 1.2 Biophysical parameters used by the BioSpec model to characterize skin specimens under normal conditions

Parameter	Value	Reference
Aspect ratio of skin surface folds	0.75	[41,42]
Thickness of stratum corneum	0.001 cm	[43]
Thickness of epidermis	0.01 cm	[43]
Thickness of papillary dermis	0.01 cm	[44]
Thickness of reticular dermis	0.1 cm	[44]
Radius of collagen fibers	25 nm	[45]
Concentration of eumelanin in the melanosomes	80 g/L	[39,46]
Concentration of pheomelanin in the melanosomes	5.2 g/L	[47]
Concentration of β-carotene in the stratum corneum	2.1e-4 g/L	[48]
Concentration of β-carotene in the epidermis	2.1e-4 g/L	[48]
Concentration of β-carotene in the blood	7.0e-5 g/L	[48]
Concentration of bilirubin in the blood	0.05 g/L	[49]
Concentration of oxy/in the blood	147 g/L	[50]
Ratio of oxy/deoxyhemoglobin	75%	[51]
Concentration of methemoglobin in the blood	1.5 g/L	[52]
Concentration of carboxyhemoglobin in the blood	1.5 g/L	[53]
Concentration of sulfhemoglobin in the blood	0 g/L	[54]
Refractive index of stratum	1.55	[55]
Refractive index of epidermis	1.4	[8]
Refractive index of papillary dermis	1.36	[56]
Refractive index of reticular dermis	1.38	[56]
Refractive index of collagen	1.5	[39]

Besides quantifying the spectral distribution of the light impinging on a skin specimen in terms of reflectance and transmittance, BioSpec also accounts for the spatial distribution of light interacting with the cutaneous tissues, which is quantified in terms of BDF. For example, Fig. 1.3 presents modeled BRDF curves

obtained using BioSpec to illustrate variations in skin glossiness associated with different values assigned to the aspect ratio (σ) of the skin surface folds, as well as the angular dependency of light reflected on the skin surface. Modeled BDF curves, in turn, can also be used in quantitative and qualitative comparisons with actual measured BDF data, thus strengthening the evaluation of the model's predictive capabilities.

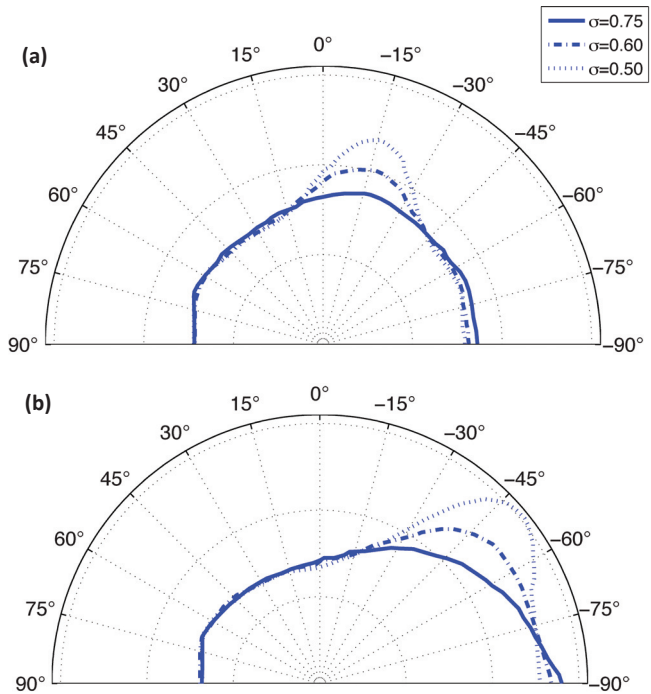

Figure 1.3 Modeled BRDF curves provided by the BioSpec model [1] depicting glossiness variations associated with different values assigned to the aspect ratio (σ) of the surface folds, and considering two angles (θ_i) of incidence. (a) θ_i = 15°, (b) θ_i = 45°.

It is worth remarking that although BioSpec provides as output bidirectional readings, one can obtain directional-hemispherical quantities by integrating the propagated light (rays) with respect to the propagation (collection) hemisphere [37]. Similarly, bihemispherical quantities can be calculated by integrating bidirectional values with respect to incident and collection hemispheres [40].

These aspects in conjunction with its algorithmic nature, make the incorporation of the BioSpec multilayered skin model into existing rendering systems straightforward. Accordingly, it can be effectively employed to generate realistic images depicting the appearance attributes of human skin (Fig. 1.4).

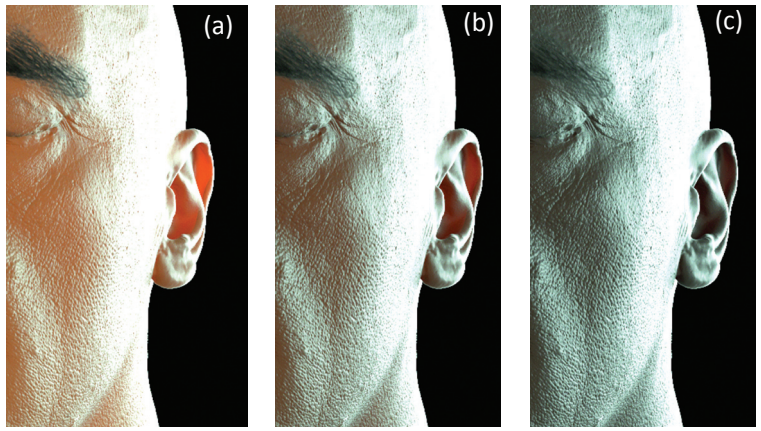

Figure 1.4 Computer-generated images illustrating color and translucency variations resulting from different levels of melanin pigmentation associated with distinct percentages of melanosomes (ϑ_m) present in the epidermis tissue. (a) ϑ_m = 3.6%, (b) ϑ_m = 10%, (c) ϑ_m = 20%. These images were rendered using a path-tracer algorithm [2] and skin spectral predictions provided by the BioSpec model (Head polygonal mesh courtesy of XYZ RGB Inc.).

1.4.3 Reproducibility

The BioSpec source code and supporting simulation data (e.g., molar extinction coefficients for pigments) were made available for download [57] to ensure code transparency and the full reproducibility of the BioSpec predictions. In addition, BioSpec can be run online via a model distribution framework (Natural Phenomena Simulation Group Distributed, or simply NPSGD) [58]. Accordingly, researchers can access its web interface (Fig. 1.5), manipulate simulation parameters associated with experimental conditions (e.g., angle of incidence and spectral range) and skin characterization data (e.g., percentage of epidermis occupied by melanosomes), and receive customized simulation results (e.g., spectral directional-hemispherical reflectance curves). It is

worth mentioning that the BioSpec source code available for download corresponds to an updated "fresh" implementation. This reimplementation of the model allowed the filtering of "bugs" and the improvement of its running performance through the use of more efficient software and hardware features.

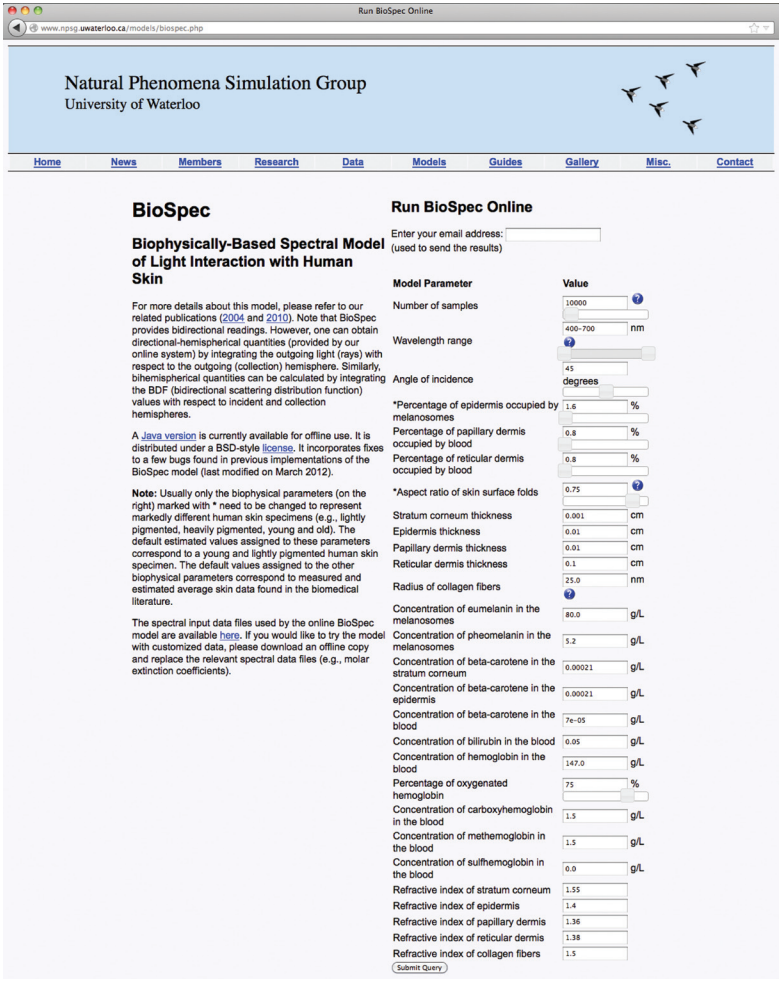

Figure 1.5 The Web interface for the BioSpec model available through the Natural Phenomena Simulation Group Distributed (NPSGD) framework [58]. Accessing this interface, researchers can configure biophysical parameters, execute light transport simulations involving different skin specimens, and receive customized results.

1.5 Future Prospects

In recent years, a substantial amount of work has been devoted to the multilayer modeling of skin appearance attributes. However, these efforts are often limited by the scarcity of measured data to characterize the optical properties of different skin specimens. Furthermore, in order to be used in a predictive manner, computer models need to be properly evaluated, which, in turn, requires comparisons of modeled data with actual measured data. Besides being also scarce, these datasets rarely include characterization data (e.g., thickness, refractive indexes, …) for the specimens employed in the measurements. The absence of this information further impairs the proper evaluation of modeled predictions. Clearly, to overcome these hurdles, it is essential to enhance quantitatively and qualitatively the measurement and dissemination of fundamental biophysical skin data.

From a scientific point of view, the modeling of skin appearance attributes is far from being a solved problem. In fact, there are a number of relevant topics that remain largely unexplored by the skin research community. For example, most current models work on the visible domain. However, there is a wide range of applications outside this domain. Noteworthy examples include the accurate modeling of appearance changes due excessive light exposure, such as tanning and photoaging, which involve predictive simulations of light and skin interactions in the ultraviolet and infrared domains, respectively. Furthermore, the biophysical characteristics of important tissue constituents, such as the size, shape, orientation, and distribution of melanosomes, are rarely taken into account in current simulation frameworks.

Finally, we believe that interdisciplinary collaborations supported by accessible data resources and code transparency can lead to significant advances in this area. After all, a well-designed model is of little use without reliable data, and code disclosure is instrumental not only for the reproduction of research results but also for the refinement of the corresponding simulation algorithms.

References

1. Krishnaswamy A and Baranoski G (2004). A biophysically-based spectral model of light interaction with human skin, *Comput Graph Forum,* **23**(3), 331–340.

2. Baranoski G and Krishnaswamy A (eds) (2010). *Light and Skin Interactions Simulations for Computer Graphics Applications,* Morgan Kaufmann, Amsterdam.
3. Baranoski G, Chen T, Kimmel B, Miranda E, and Yim D (2012). On the noninvasive optical monitoring and differentiation of methemoglobinemia and sulfhemoglobinemia, *J Biomed Opt,* **17**(9), 097005-1–097005-14.
4. Cavalcanti P, Scharcanski J, and Baranoski G (2013). A two-stage approach for discriminating melanocytic skin lesions using standard cameras, *Expert Syst Appl,* **40**(10), 4054–4064.
5. Hunter R and Harold R (eds) (1987). *The Measurement of Appearance*, 2nd ed., Wiley-Interscience, New York.
6. Nicodemus FE, Richmond JC, Hsia JJ, Ginsberg IW, and Limperis T (1992). Geometrical considerations and nomenclature for reflectance, in *Physics-Based Vision Principles and Practice: Radiometry* (Wolf LB, Shafer SA, and Healey GE, eds), Jones and Bartlett Publishers, Sudbury, pp. 94–145.
7. Prahl S (1988). *Light Transport in Tissue*, Ph.D. thesis, The University of Texas at Austin, TX, USA.
8. Tuchin V (ed) (2007). *Tissue Optics: Light Scattering Methods and Instruments for Medical Diagnosis*, SPIE PM (SPIE/International Society for Optical Engineering).
9. Kubelka P and Munk F (1931). Ein beitrag zur optik der farbanstriche, *Zurich Tech Phys,* **12**, 593–601.
10. Anderson R and Parrish J (1981). The optics of human skin, *J Invest Dermatol,* **77**(1), 13–19.
11. Wan S, Anderson R, and Parrish J (1981). Analytical modeling for the optical properties of the skin with in vitro and in vivo applications, *Photochem Photobiol,* **34**, 493–499.
12. Doi M and Tominaga S (2003). Spectral estimation of human skin color using the Kubelka–Munk theory, in *SPIE/IS&T Electronic Imaging* (SPIE, vol 5008), pp. 221–228.
13. Donner C and Jensen H (2005). Light diffusion in multi-layered translucent materials, *ACM T Graphic,* **24**(3), 1032–1039.
14. Ishimaru A (ed) (1978). *Wave Propagation and Scattering in Random Media*, vol 1, 2nd ed., IEEE Press, New York.
15. van Gemert M, Welch A, Star W, Motamedi M, and Cheong W (1987). Tissue optics for a slab geometry in diffusion approximation, *Laser Med Sci,* **2**, 295–302.

16. Farell T, Patterson M, and Wilson B (1992). A diffusion theory model of spatially resolved, steady-state diffuse reflectance for the noninvasive determination of tissue optical properties in vivo, *Med Phys,* **19**, 879–888.
17. Hielscher A, Alcouffe R, and Barbour R (1998). Comparison of finite-difference transport and diffusion calculations for photon migration in homogeneous tissues, *Phys Med Biol,* **43**, 1285–1302.
18. Chen B, Stamnes K, and Stamnes J (2001). Validity of the diffusion approximation in bio-optical imaging, *Appl Opt,* **40**(34), 6356–6336.
19. Sardar D and Levy L (1998). Optical properties of whole blood, *Laser Med Sci,* **13**, 106–111.
20. Steinke J and Shepherd A (1988). Diffusion model of the optical absorbance of whole blood, *J Opt Soc Am,* **5**(6), 813–822.
21. Flock S, Patterson M, Wilson B, and Wyman D (1989). Monte Carlo modeling of light propagation in highly scattering tissues—I: model predictions and comparison with diffusion theory, *IEEE T Biomed Eng,* **36**(12), 1162–1168.
22. Yoon G, Prahl S, and Welch A (1989). Accuracies of the diffusion approximation and its similarity relations for laser irradiated biological media, *Appl Opt,* **28**(12), 2250–2255.
23. Donner C and Jensen H (2006). A spectral BSSRDF for shading human skin, in *Rendering Techniques 2006: 17th Eurographics Workshop on Rendering*, pp. 409–418.
24. Donner C, Weyrich T, d'Eon E, Ramamoorthi R, and Rusinkiewicz S (2008). A layered, heterogeneous reflectance model for acquiring and rendering human skin, *ACM T Graphic,* **27**(5), 140:1–140:12.
25. Prahl S, van Gemert M, and Welch A (1993). Determining the optical properties of turbid media using the adding-doubling method, *Appl Opt,* **32**(4), 559–568.
26. Nielsen K, Zhao L, Stamnes J, Stamnes K, and Moan J (2004). Reflectance spectra of pigmented and nonpigmented skin in the UV spectral region, *Photochem Photobiol,* **80**, 450–455.
27. Stamnes K, Tsay S-C, Wiscombe W, and Jayaweera K (1988). Numerically stable algorithm for discrete-ordinate-method radiative transfer in multiple scattering and emitting layered media, *Appl Opt,* **27**(12), 2502–2509.
28. Chandrasekhar S (ed) (1960). *Radiative Transfer,* Dover Publications Inc., New York.

29. Hammerley J and Handscomb D (eds) (1964). *Monte Carlo Methods,* Wiley, New York.

30. Shimada M, Yamada Y, Itoh M, and Yatagai T (2001). Melanin and blood concentration in human skin studied by multiple regression analysis: assessment by Monte Carlo simulation, *Phys Med Biol,* **46**, 2397–2406.

31. Wang L, Jacques S, and Zheng L (1995). MCML–Monte Carlo modeling of light transport in multi-layered tissues, *Comput Meth Prog Bio,* **47**, 131–146.

32. Nishidate I, Aizu Y, and Mishina H (2004). Estimation of melanin and hemoglobin in skin tissue using multiple regression analysis aided by Monte Carlo simulation, *J Biomed Opt,* **9**(4), 700–710.

33. Prahl S, Keijzer M, Jacques S, and Welch A (1989). A Monte Carlo model of light propagation in tissue, in *SPIE Proceedings of Dosimetry of Laser Radiation in Medicine and Biology*, vol IS 5 (Müller G and Sliney D, eds), pp. 102–111.

34. Trowbridge T and Reitz K (1975). Average irregularity representation of a rough surface for ray reflection, *J Opt Soc Am,* **65**(5), 531–536.

35. Bruls W and van der Leun J (1984). Forward scattering properties of human epidermal layers, *Photochem Photobiol,* **40**, 231–242.

36. McCartney E (ed) (1976). *Optics of the Atmosphere: Scattering by Molecules and Particles,* John Wiley & Sons Inc., New York.

37. Baranoski G, Rokne J, and Xu G (2001). Virtual spectrophotometric measurements for biologically and physically-based rendering, *Visual Comput,* **17**(8), 506–518.

38. Vrhel M, Gershon R, and Iwan L (1994). The measurement and analysis of object reflectance spectra, *Color Res Appl,* **19**(1), 4–9.

39. Jacques S (1996). Origins of tissue optical properties in the UVA, visible, and NIR regions, in *OSA TOPS on Advances in Optical Imaging and Photon Migration* (Alfano RR, and Fujimoto JG, eds), vol 2, pp. 364–369.

40. Krishnaswamy A, Baranoski G, and Rokne J (2004). Improving the reliability/cost ratio of goniophotometric measurements, *J Graph Tool,* **9**(3), 31–51.

41. Magnenat-Thalmann N, Kalra P, Lévêque J-L, Bazin R, Batisse D, and Querleux B (2002). A computational skin model: fold and wrinkle formation, *IEEE T Inf Technol B,* **6**(4), 317–323.

42. Talreja P, Kasting G, Kleene N, Pickens W, and Wang T-F (2001). Visualization of the lipid barrier and measurement of lipid pathlength in human stratum corneum, *AAPS Pharmsci,* **3**(2), 48–56.

43. Gambichler T, Boms S, Stücker M, Kreuter A, Moussa G, Sand M, Altmeyer P, and Hoffmann K (2006). Epidermal thickness assessed by optical coherence tomography and routine histology: preliminary results of method comparison, *J Eur Acad Dermatol,* **20**(7), 791–795.

44. Agache P (2004). Main skin physical constants, in *Measuring the Skin* (Agache P and Humbert P, eds), Springer-Verlag, Berlin, pp. 747–757.

45. Li S (2003). Biologic biomaterials: tissue-derived biomaterials (collagen), in *Biomaterials Principles and Applications* (Park J and Bronzano J, eds), CRC Press, Boca Raton, pp. 117–139.

46. Kollias N and Baqer A (1986). On the assessment of melanin in human skin in vivo, *Photochem Photobiol,* **43**(1), 49–54.

47. Hennessy A, Oh C, Diffely B, Wakamatsu K, Ito S, and Rees J (2005). Eumelanin and pheomelanin concentrations in human epidermis before and after UVB irradiation, *Pigm Cell Res,* **18**(3), 220–223.

48. Lee R, Mathews-Roth M, Pathak M, and Parrish J (1975). The detection of carotenoid pigments in human skin, *J Invest Dermatol,* **64**(3), 175–177.

49. Martin C and Cloherty J (2008). Neonatal hyperbilirubinemia, in *Manual of Neonatal Care* (Cloherty J, Eichenwald E, and Stark A, eds), Wolters Kluwer, Philadelphia, pp. 181–212.

50. Yaroslavsky A, Priezzhev A, Rodriquez J, Yaroslavsky I, and Battarbee H (2002). Optics of blood, in *Handbook of Optical Biomedical Diagnostics* (Tuchin V, ed), SPIE-Press, pp. 169–216.

51. Öberg P (2003). Optical sensors in medical care, *Sens Update,* **13**(1), 201–232.

52. Haymond S, Cariappa R, Eby C, and Scott M (2005). Laboratory assessment of oxygenation in methemoglobinemia, *Clin Chem,* **51**(2), 434–444.

53. Cunnington A, Kendrick S, Wamola B, Lowe B, and Newton C (2004). Carboxyhemoglobin levels in Kenyan children with plasmodium falciparum malaria, *Am J Trop Med Hyg,* **71**(1), 43–47.

54. Yarynovska IH and Bilyi AI (2006). Absorption spectra of sulfhemoglobin derivatives of human blood, in *Optical Diagnostics and Sensing VI* (Cote G and Priezzhev A, eds), SPIE, pp. 1–6.

55. Diffey B (1983). A mathematical model for ultraviolet optics in skin, *Phys Med Biol,* **28**(6), 647–657.

56. Jacques S, Alter C, and Prahl S (1987). Angular dependence of HeNe laser light scattering by human dermis, *Laser Life Sci,* **1**, 309–333.

57. NPSG (2011). Run BioSpec Online, School of Computer Science, University of Waterloo, http://www.npsg.uwaterloo.ca/models/biospec.php.

58. Baranoski G, Dimson T, Chen T, Kimmel B, Yim D, and Miranda E (2012). Rapid dissemination of light transport models on the web, *IEEE Comput Graph*, **32**, 10–15.